 IEEE Transactions on Nuclear Science, Vol. NS-32, No. 5, October 1985

FERRITE KICKER MAGNET FOR THE LAMPF SWITCHYARD UPGRADE*

R. A. Hardekopf, E. F. Higgins, and J. S. Lunsford, AT-3, MS H808
Los Alamos National Laboratory, Los Alamos, NM 87545 USA

Summary

The new LAMPF switchyard requires a kicker magnet as the first element in the transport line leading to the Proton Storage Ring (PSR). The magnet must produce 1-ms-long pulses with 40-μs rise time and <0.3% flat-top regulation to deflect the 800-MeV H^- beam by 1.2°. We have constructed two 1-m-long, single-turn ferrite magnets, each powered by a modulator supplying up to 2400 A at a maximum rate of 24 Hz. The modulators use a transistor amplifier/regulator, a dual pulse-forming-network (PFN), and a compensating circuit driven by a function generator to achieve a total 0.1% current variation in the pulse. The system also produces an alternate kicking mode consisting of 150-μs-long pulses at a maximum rate of 120 Hz; the two modes can be multiplexed within the charging power-supply limitations.

Introduction

The PSR is an addition to the Weapons Neutron Research (WNR) neutron-spallation facility at LAMPF. The PSR acts as a bunch compressor for the relatively long (~1 ms) linac macropulses, tailoring them into short (~0.3 μs), intense pulses suited for neutron scattering research. In the LAMPF switchyard area, beams are directed into the major experimental areas, with high-intensity negative beam bent into Line D (PSR/WNR) by the kicker magnet and a septum magnet.

A variety of beam patterns can be produced for Line D and PSR, placing different timing requirements on the kicker magnet.[1] For those cases where entire LAMPF macropulses (up to 1 ms long) are deflected to PSR, the rise time of the kicker is not critical. For other experimental requirements where only part of a macropulse is needed, it is desirable to keep the rise time of the kicker as short as possible, allowing the first part of the macropulse to be used in other LAMPF experimental areas. A time of 40 μs was chosen as a reasonable compromise between beam efficiency and driver capability.

The repetition-rate specification originally was set by the two design modes of PSR operation, 12 Hz for long-bunch and 120 Hz for short-bunch mode. The long-bunch kicker rate specification was increased to 24 Hz to permit doubling the PSR average current. The kicker pulse-lengths of 1 ms at 24 Hz, or 150 μs at 120 Hz, yield roughly equal duty factors of 2.5%.

Magnet Optics Requirements

The Line D transport line is 90 m in length from the switchyard kicker magnet to the beginning of the PSR injection line. The 60-m long injection line provides halo and energy dispersion scraping prior to focusing the H^- ions at a magnetic stripper located just before the ring. Spatial uniformity and time-structure specifications for the kicker magnet are determined largely by the stringent requirements of this injection line.

The primary effect of a kicker field inhomogeneity is to shift the beam-halo centroid relative to the beam core, causing an effective emittance growth. A limit of 0.3% is placed on the variation of integrated B-field at seven times the rms beam radius along the beam trajectory through the magnet. By constructing the kicker magnet in two segments and centering each segment about the average kicked-beam trajectory, we could meet the field specification with a 5 x 10 cm aperture.

The more difficult specification to achieve is the temporal field uniformity. A maximum 0.1% rms amplitude variation over the 1-ms-long flat top of the magnetic field is imposed from calculated emittance growth at the injection point of the PSR. A maximum peak amplitude variation of 0.3% during the pulse or from pulse-to-pulse is imposed from beam-spill and aperture-clearance considerations.

Magnet Design

The fast rise time, variable pulse length, high duty factor, spatial uniformity, and high degree of amplitude regulation required by the kicker magnet were important considerations in the design.[2] We chose a single-turn conductor, lumped-inductance ferrite magnet for the basic element. To produce the required field with a current in the range of 2 kA (where solid-state regulator circuits are applicable) and at the same time to keep the load inductance and peak voltage at low values, we constructed separate drivers for the two magnet sections.

Mechanical construction of each section employs a 1-m-long stack of ferrite blocks (see Fig. 1). The window-frame aperture has recesses at the conductors to achieve better field uniformity and to provide for precise conductor alignment. Ceramic rails hold the copper bars in place along the length of the magnet. Each unit has a calculated inductance of 3 μH, and together yield a 1.2° kick for 2-kA current.

Transient effects were investigated with respect to current distribution in the conductors, hysteresis and eddy-current losses in the ferrite, remanent air-gap field, and conductor resistive losses.[2] The most significant heat losses occur in the conductors. Because the use of ceramic chambers in the LAMPF switchyard was not advised, we elected to place the entire magnet assembly inside a vacuum container. We provided conductor cooling only in the electrical

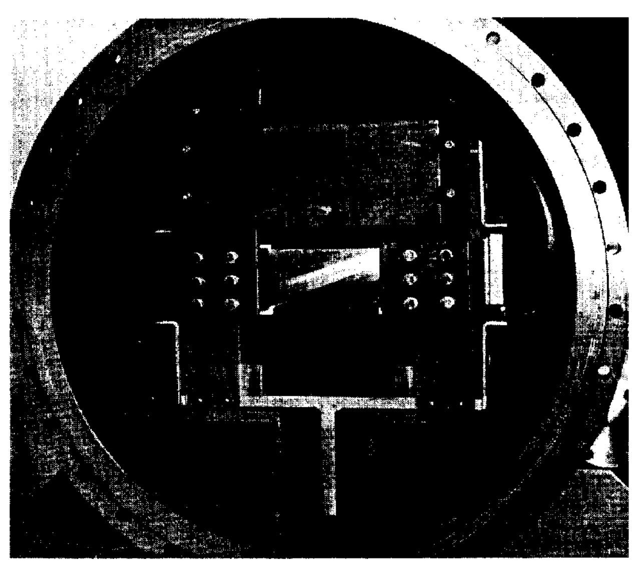

Fig. 1. Kicker magnet unit in vacuum chamber.

*Work supported by the US Dept. of Energy.

feedthroughs at one end of the magnet. An oversize end connection at the opposite end provided some radiative heat loss to the end flange, and both surfaces were blackened with an Ebonol treatment to enhance this effect. The connecting straps were annealed, polished on the mating surfaces, and clamped with steel nut plates to provide good heat transfer in vacuum. At the full repetition rate, maximum temperature rise across the conductors was about 34°C with an ad-ditional 10°C between the cooled feedthroughs and the connecting straps.

Modulator Design

The modulator design uses a three-loop current driver to supply current to the kicker magnet (see Fig. 2). The circuit uses a high-current transistor amplifier in conjunction with a dual PFN to establish, sustain, and regulate the current wave. The transistor amplifier/regulator and the dual PFN share in the overall current development; the amplifier supplies about 10% of the total while the PFNs supply the remainder. Active feedback is used in the amplifier/regulator to deripple the PFN contribution and to provide a constant current to the kicker during the required pulse interval. Adjustment of the pulse length is achieved by a PFN line-length-changing circuit that couples appropriate sections of the PFN through semiconductor switches. Kicker magnetic-field level is set by adjusting the PFN charge voltage and a reference voltage level supplied to the feedback circuit.

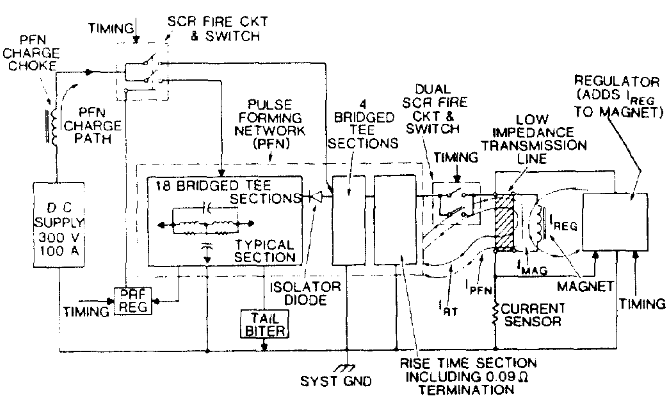

Fig. 2. Functional diagram of the modulator, showing three current loops through the magnet.

Pulse Forming Network

A terminated PFN was chosen to provide the required 40-μs rise time and the major portion (>90%) of the required 2000-A magnet current with good amplitude repeatability and reliability. The PFN impedance (0.1 Ω) was chosen as low as feasible to keep power dissipation and voltage stress to a minimum. Most of the PFN consists of identical bridged-T sections similar to the constant-impedance circuits used in distributed amplifier designs. Use of the bridged-T circuit resulted in a PFN that could be shortened or lengthened, without affecting ripple, by simply deleting or adding identical sections.

To obtain 40-μs rise time while maintaining a minimum PFN impedance required use of a special rise-time section. The placement of the terminating resistor was critical for stable operation of the flat-top regulating circuit. It was also necessary for stable regulator operation to add phase-enhancing snubber circuits across the transmission line. As shown in Fig. 2, two parallel SCRs are used to discharge the PFN into the magnet, each SCR carrying the full current on alternate pulses.

For short-pulse (150-μs) operation the rise-time section and four bridged-T sections are charged through the short-pulse resonant charging circuit. An isolator diode prevents charging of the remainder of the PFN. For long-pulse (1-ms) operation, the entire PFN is charged through the long-pulse resonant charging circuit. For long-pulse operation, a tail-biter circuit is used to decrease the pulse fall time rapidly to assure zero current flow in the magnet when the next beam pulse passes through the magnet. Resonant charging circuits were chosen to charge the PFN because of their efficiency and the ease of precise voltage voltage regulation using de-Q circuitry.[3] Precise PFN voltage regulation (0.1%) is required to meet pulse-to-pulse requirements because the flat-top current regulator uses the first current peak as a reference for the pulse regulation.

Regulator

Although the PFN described above was designed to minimize losses, some loss is inherent in the inductors and capacitors. The PFN assembly thus becomes a lumped-element approximation to a finite length of charged distributed line; thus both ripple and droop errors occur in the load current. These errors were measured on a prototype PFN and amounted to 3.3% rms ripple and 10.4% droop at the end of a 1-ms pulse. The regulation method employs active feedback and supplies current in proportion to the difference between a reference value and the actual magnet current. The reference point is established by a low-droop, track-and-hold circuit gated to hold at the peak value of the rising current edge. Thus, the regulator adds varying amounts of current all along the active part of the kick cycle.

In Fig. 3, R(s) is the reference signal, E(s) represents the actuating signal, B(s) is the primary feedback signal, and C(s) is the controlled current variable. Factors $G_1(s)$, $G_2(s)$, and H(s) represent the usual transfer functions associated with a feedback servo system. The ΔI factor represents a disturbance in the magnet load current such as ripple or droop. The X represents the separation point in the low-level part of the circuit where the open-loop transfer function, B(s)/E(s), can be measured. The feedback circuit can be analyzed by relating C(s) to R(s) in the closed-loop connection (X closed) as follows:

$$C(s) = G_2(s)\left[\frac{G_1(s)R(s)}{1 + G_1(s)G_2(s)H(s)} + \frac{\Delta I}{1 + G_1(s)G_2(s)H(s)}\right]$$

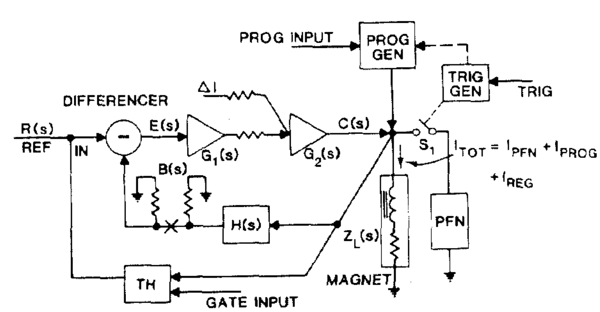

Fig. 3. Active feedback regulator functional diagram.

The closed-loop expression above reveals that errors in the desired current and load fluctuations represented by ΔI are each reduced by $[1 + G_1(s) G_2(s) H(s)]$, the open-loop gain factor plus 1. This fact can be used to establish the magnitude of the open-loop response needed for reducing the magnet ripple and droop errors. In Fig. 4, the measured gain values are plotted on a Bode gain diagram along with several other pertinent feedback-system parameters.

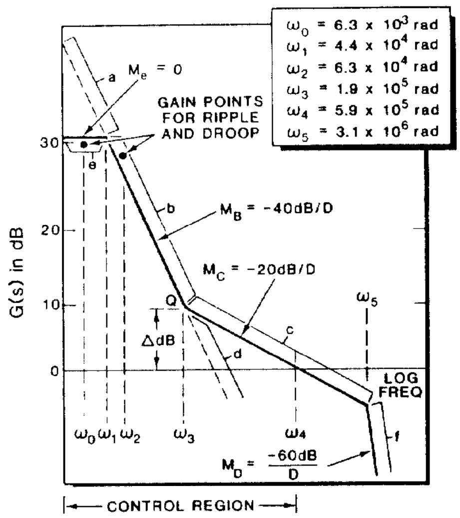

Fig. 4. Bode diagram for the regulator. Abscissa (frequency) is not to scale.

Three possible design options for shaping the overall gain response are shown in Fig. 4 (that is, response paths abd, ebcf, and abcf). We chose the Bode asymptotic response approximation ebcf because options abd or abcf would have caused difficulty in overload, settling time, open-loop measurement instabilities from the extremely high dc gain in the forward-loop path, or a lack of phase margin that is due to $|G(s)|$ having a large slope (-40 dB/decade) at ω_4, the gain crossover frequency. The chosen response has the advantage of relatively large bandwidth coupled with a favorable (-20 dB/decade) slope through the ω_4 crossover, which considerably reduces the phase slope.

The overall response G(s) for the system (see Fig. 4) becomes

$$G(s) = 34\left[\frac{(1 + s/1.9 \times 10^5)}{(1 + s/4.4 \times 10^4)^2(1 + s/3.1 \times 10^6)^3}\right] .$$

This function was implemented with the aid of two operational amplifiers, a 500-A current driver amplifier, and several RC frequency compensation networks within the amplifier circuits. The measured open-loop gain for the system was 30.6 dB at 1 kHz and 27.5 dB at 10 kHz, providing overall droop reduction to 0.3%, and ripple reduction to 0.13% (see Fig. 5).

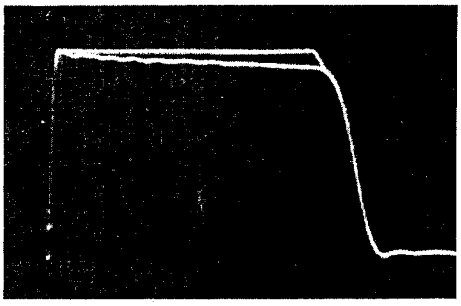

Fig. 5. Switchyard kicker PFN current with (upper trace) and without feedback applied (200μs/division, 500 A/division).

The measured gain margin was 8 dB with a phase margin of 44°, factors that represent acceptable stability margins.

To improve performance, a second current-injection amplifier (PROG GEN) was added to the circuit as shown in Fig 3. This amplifier was then driven by a gated arbitrary-function generator having 10-bit programming capability. Using a 100-point function, approximately 7-bits, the current errors were reduced to 1 A rms at the 2000-A current level (Fig. 6). Thus, 0.05% rms regulation was achieved, and with greater bit densities we estimate that this technique could achieve performance of 0.1 A rms or 0.005% regulation.

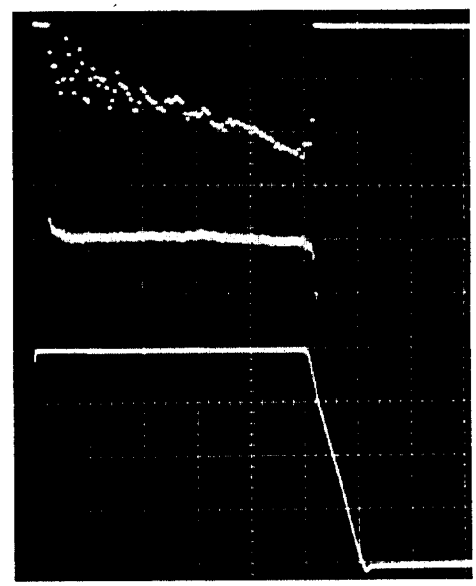

Fig. 6. Final pulse shape with applied function generator. The 100-point function applied is shown at the top at 2 V/division. The lower trace is the final pulse (200 μs/division, 500 A/division), and the middle trace is an expanded view of the flat top at 5 A/division.

Conclusion

The kicker magnets have been constructed and installed in the LAMPF switchyard. The modulators have been tested at full duty factor and meet the 40-μs rise time, 1-ms flat top, and the 0.3% regulation specifications. In fact, when the programmable function (feedforward) is added to the regulating circuit, a current variation of less than 0.1% is achieved. The project demonstrates the impact of feedback and programmed error-reduction technology on kicker regulation.

Acknowledgments

We gratefully acknowledge the contributions of Andrew Jason to the optics specifications, and Klaus Metzmacher to the magnet design and calculations. The effort of Laybe Torres and Lloyd Feind in construction, testing, and installation of the system is deeply appreciated.

References

1. R. A. Hardekopf, "PSR Beam-Pulse Formation and Control," Proc. Seventh Meeting of the Int. Collaboration on Advanced Neutron Sources, (ICANS-VII), AECL-8488 (September 1983), 134.
2. Klaus Metzmacher, "Design Proposals for a New Switchyard Kicker Magnet," PSR Technical Note No. 105, May 1982 (unpublished).
3. E. F. Higgins, "Switchyard Kicker Pulse-Forming-Network Charging System and DC Power-Supply Ratings," PSR Technical Note No. 123, July 1984 (unpublished).